

AD-A199 378

(4)

Final Technical Report

N00014-84-K-0500

July 1, 1984 - September 30, 1987

"Low Reynolds Number - Separation Bubble"

Principal Investigators: Robert Liebeck and Ron Blackwelder

Scientific Officer: S. Lekoudis

DTIC
SELECTED
AUG 31 1988
S H D

Introduction and Goals.

The aim of this research has been to investigate the flowfield details and global performance characteristics of the transitional separation bubble which typically occurs near the onset of an adverse pressure gradient on airfoils operating at low Reynolds numbers.

Earlier research on the problem by various investigators has shown the laminar separation bubble to follow a typical sequence of events: the separation of a laminar boundary layer due to deceleration in the adverse pressure gradient region; the growth of a laminar separated shear layer and inviscid instabilities associated with the shear layer; transition from laminar to turbulent flow; increased mixing, entrainment of higher speed fluid and the corresponding growth of a turbulent separated shear layer; and finally reattachment of the turbulent shear layer and the development of a turbulent boundary layer. Previous studies have also indicated that the presence of a laminar bubble on an airfoil can lead to a degradation of performance, especially an increase in the drag coefficient as compared with that measured at a higher Reynolds number or with a boundary layer trip. In both

DISTRIBUTION STATEMENT A

Approved for public release;
Distribution unlimited

cases boundary layer transition occurs upstream of the separation point precluding the formation of a laminar separation bubble, and the flow remains attached. These results have also shown that increases in the size or extent of the separation region correlate with increases in drag for a particular airfoil incidence. Thus, the present investigation of the flowfield structure associated with the separation bubble phenomenon has been made to examine in more detail the manner in which the bubble affects drag. An investigation has also been made of the effects of external forcing, including free stream turbulence and acoustic disturbances, on the separated flow and transition, since these parameters can lead to changes in performance and may be used to illustrate the effects of the laminar bubble.

Summary of Work Accomplished.

Experiments in the present investigation have concentrated on the flowfield and performance of an LA2573A airfoil operating at chord Reynolds numbers near 250,000. This flow condition is in the lower band of the design range for the airfoil, where adverse effects of the separation bubble were previously shown to be most significant. A sketch of the test airfoil and its design pressure distribution is included in figure 1.

Global airfoil performance including lift and drag measurements were obtained through pressure distribution measurements around the airfoil contour and through a scan of wake pressures used in computing drag coefficients. Airfoil performance measurements were used for comparisons between cases with forced or unforced external disturbances and also to check the current results against measurements previously obtained in tests at Douglas Aircraft Co.



✓	
<i>per letter</i>	
Dist	2
A-1	

More detailed flowfield measurements were obtained through measurements of velocity in the airfoil boundary layer with a constant temperature hot-wire anemometer. Results included mean velocity boundary layer profiles at chordwise stations ranging from upstream of the laminar separation bubble to the trailing edge on the upper surface. Integral length parameters associated with these profiles, including the displacement thickness (δ^*) and the momentum thickness (θ) have also been computed. Turbulent intensity profiles have been recorded to give a better indication of the transition position, and spectral measurements of the instantaneous velocity signal within the boundary layer have been found to indicate peak fluctuation frequencies associated with boundary layer instabilities which lead to transition.

Investigation of the effects of external forcing included cases with an increase in the free stream turbulence which was produced by a coarse grid positioned over 60 mesh lengths upstream of the airfoil model. With a wire diameter of 0.12 in., the grid produced a turbulence intensity of approximately .9% at the model location. As a result of the increased free stream fluctuations, a thinner laminar separation bubble and downstream turbulent boundary layer, earlier transition within the bubble and an overall reduced drag were noted when compared with measurements obtained at the nominal tunnel conditions with a turbulence level of approximately .1%.

Some initial results with global acoustic forcing indicated some effects similar to those associated with the increase in free stream turbulence; however, measurements have suggested that such forcing applied at discrete frequencies only affects the laminar separation bubble at forcing frequencies in the region of the instability peak previously noted from measurements of boundary layer velocity spectra.

Details of results from this experimental investigation of the laminar separation bubble on an airfoil at low Reynolds number may be found in the three annual letter reports submitted over the duration of contract N00014-84-K-0500 for the 1985, 1986, and 1987 fiscal years. (These reports are indexed on page 10.) Meanwhile, some highlights of these measurements will be included in this final summary to illustrate results which contributed to some final conclusions.

In addition to wind tunnel measurements, a new towing tank facility has been constructed in order to allow flow visualization of the LA2573A airfoil flowfield at chord Reynolds numbers around $.25 \times 10^6$ for comparison with flow measurements. The aim of this new facility was to improve upon some preliminary visualization results obtained in a much smaller tank with limited Reynolds number capability. While the larger towing tank has recently been completed, experimental results were not yet available at the expiration of this contract.

Apparatus.

Wind tunnel measurements were made in the USC Dryden tunnel, a closed return facility with a maximum test section velocity of approximately 34 m/s. The model consisted of a numerically milled, pressure tapped aluminum airfoil section with a 6 inch chord and 38 inch span which was adapted with 8 inch balsa extensions to span the 54 inch wide USC tunnel. A computer controlled traverse was used for positioning of the wake rake for pressure measurements and the single hot-wire probe for boundary layer velocity measurements. Some further details associated with the experimental apparatus and procedures may be found in the three Year-End Technical Reports indexed on page 10, and in publication [1],

listed on page 10.

Highlights of Results.

A summary of global airfoil performance at $R_c = .25 \times 10^6$ is presented in figure 2. The lift curve remains constant for the various tunnel configurations, and drag coefficients measured in the USC tunnel at the baseline free stream turbulence correspond quite well to measurements made previously on the same airfoil in the Douglas tunnel. Both facilities have approximately the same turbulence level, and although the free stream velocity spectra differ in general, the fluctuation levels appear to be similar at frequencies in the range where boundary layer instabilities have been observed. Measurements with the increased turbulence configurations in the USC tunnel indicate a significant decrease in drag in the vicinity of the design lift coefficient ($C_l = .68$). A sample comparison between pressure distributions obtained at USC and Douglas was also provided in the FY'85 report to demonstrate the good agreement between results from the two facilities. In addition, measurement of the wake drag at different span positions indicated that any variations in the drag coefficient were within the experimental error. This observation in the FY'87 report implied the absence of any global three dimensional effects present in the experimental results.

Measurement of velocities within the boundary layer provide a more detailed description of the evolution of the laminar separation bubble flowfield. Figures 3 and 4 present a sample progression of mean velocity and turbulent intensity profiles measured in the boundary layer at $R_c = .23 \times 10^6$ and $\alpha = 8^\circ$ ($C_l = .93$) with a clean tunnel configuration. These measurements are similar to those presented in the FY'85 report for $\alpha = 0^\circ$ and 5° . At

chord position $x/c = .223$, the boundary layer remains attached and laminar. The laminar profile at $x/c = .279$ shows the boundary layer at a point near separation, and profiles at $x/c = .328$ and $.356$ illustrate the development of the separation region. It is noted that although reverse flow is probable at these locations, the output of the hot-wire anemometer will only produce a rectification or absolute value of the velocity signal at best. Thus, profiles in this region primarily provide an indication of the extent of the boundary layer separation as evidenced by the constant low magnitude portion of the profile near the wall. Along the airfoil surface up to $x/c = .356$, low values at points in the turbulent intensity profiles of figure 4 have indicated a laminar flow; however, at chord position $x/c = .383$, the turbulent intensity has increased significantly, indicating transition. Evidence for transition can also be seen by the increased magnitude of the mean velocity profile in the separated region at this location. The boundary layer at $x/c = .411$, where the mean velocity profile begins to show a gradient in the region close to the wall, marks the approximate location of reattachment, and a profile at $x/c = .449$ represents a typical turbulent boundary layer in an adverse pressure gradient. It was noted in the FY'85 report that the influence of the tunnel traverse used in obtaining hot-wire measurements had a negligible effect on the airfoil flowfield.

An example of the spectral development of the boundary layer is arranged in a chordwise progression in figure 5 for a clean tunnel at $R_c = .23 \times 10^6$ and $\alpha = 8^\circ$. (Refer to figures 3 and 4 for corresponding boundary layer profiles at the same configuration.) Spectra were measured at a location in the boundary layer where the mean velocity is equal to approximately 70% of the edge velocity. This position was chosen because it corresponds to the location of the maximum fluctuation level in the separated boundary layer. The

series begins with the spectrum of a velocity signal in the attached laminar region at chord position $x/c = .248$. A pronounced instability peak is found around 3.7 kHz for the spectra at $x/c = .356$ and $.383$, where the separated boundary layer nears transition. A higher harmonic around 7.5 kHz is also evident at the latter position. Finally, a fully turbulent boundary layer spectrum is seen at $x/c = .411$ where the boundary layer approaches reattachment, and this is compared with the spectrum from a well developed turbulent profile near the trailing edge at $x/c = .990$. The above results are significant because the local peak in the spectrum in the separated region was found to correspond to the most amplified frequency in a separated shear layer. Thus, the mode for transition seems to be characterized by a free shear layer instability.

In examining the effects of an increase in the free stream turbulence, boundary layer data provided some additional clues to explain the decrease in drag which was found in figure 2. The contour of distances at which the boundary layer velocity measured 30% of the edge velocity (defined here as the separation thickness) was plotted in figure 6 to indicate an estimate for the size and extent of the separation region. Data is included for airfoil incidences of 0° , 4° and 8° , and bubble profiles at all angles show a reduction in thickness and an earlier transition and reattachment due to an increase in free stream turbulence. Differences are most dramatic at 8 degrees where the drag coefficient was most noticeably decreased (see figure 2). Also, comparisons of boundary layer velocity spectra between the different free stream turbulence configurations at particular chord positions in the separated region showed a significant increase in the amplified level of the instability peak as a result of an increase in the free stream fluctuations. Additional results corresponding to the investigation of increased free stream turbulence are discussed in the

FY'86 report.

For an investigation of the effects of acoustic forcing, a mid-range loudspeaker with an approximately flat frequency response measured between 2.8 and 5.3 kHz was mounted opposite the airfoil lifting surface. The extent of the laminar region of the separation bubble as reflected in the length of a flat pressure plateau found in pressure distributions served as a gauge to indicate the frequency range over which acoustic forcing affected the bubble flow field. A sample comparison between forced and unforced pressure distributions was included in the FY'87 report. It was found that forcing was effective in changing the airfoil pressure distribution over approximately the same range of frequencies as the instability peak noted in the spectral plot of figure 5 at $\alpha = 8^\circ$. A reduction in drag was also measured for this case. Details of the boundary layer flow field, as given by a plot of the displacement thickness (δ^*) in figure 7, show a decrease in the boundary layer thickness beginning near separation as a result of the forcing. In addition, the velocity spectra in the transition region shows a sharp spike at the forcing frequency for the forced case in figure 8 where a broadband peak had been found in the unforced case. An apparent increase in the amplified level of boundary layer fluctuations at a particular chord position led to an earlier transition. Additional information on these acoustic forcing measurements may be obtained in the FY'87 report.

Conclusions.

Experiments have outlined the details of the flowfield structure associated with the laminar separation bubble occurring on an airfoil at low Reynolds number. In particular, boundary layer velocity spectra have revealed a peak in the frequency of velocity fluctuations

corresponding to instabilities which lead to transition within the separated shear layer.

Increases in the disturbance field external to the test model have led to a decrease in the thickness of the bubble separation region and turbulent boundary layer downstream of the bubble. An earlier transition as a consequence of forcing seemed to result from an increase in the level of amplified velocity fluctuations at a particular chord position in the laminar region of the separated shear layer and accordingly an earlier saturation of these transitional instabilities. This general result was evident from both broadband increases in the free stream turbulence level and monochromatic increases in the sound pressure level. However, in the case of acoustic forcing, only forcing frequencies in the range of the boundary layer spectral fluctuation peak were found to influence the laminar separation bubble. A comparison of airfoil performance for the different cases showed a significant decrease in drag for forcing cases where the bubble flowfield was affected.

In general, results from this investigation seem to indicate that changes in the low Reynolds number airfoil flowfield or its external environment which contribute to the amplification of flow instabilities in the laminar separation region can be used to influence the size and extent of the laminar bubble and accordingly airfoil performance.

Additional experimental work which focused on the means of interaction between external forcing and the amplification of boundary layer instabilities or a study of the amplification and transition process itself in the separated flowfield might ultimately be used to aid numerical modeling of low Reynolds number airfoil flows and allow better prediction of performance.

Index of Technical Reports.

FY'85 End-of-the-year letter; July 1,1984 - Sept. 30, 1985; N00014-84-K-0500

FY'85-S Supplement to End-of-the-year letter; July 1,1984 - Sept. 30, 1985;
N00014-84-K-0500; NR 679-012

FY'86 End-of-the-year letter; Oct. 1,1985 - Sept. 30, 1986; N00014-84-K-0500

FY'87 End-of-the-year letter; Oct. 1,1986 - Sept. 30, 1987; N00014-84-K-0500

Index of Publications.

1. P. J. LeBlanc, R. H. Liebeck, and R. Blackwelder. Boundary layer and performance characteristics from wind tunnel tests of a low Reynolds number Liebeck airfoil. In *Aerodynamics at Low Reynolds Numbers*, pages 8.1-8.19, The Royal Aeronautical Society, London, Oct. 1986.

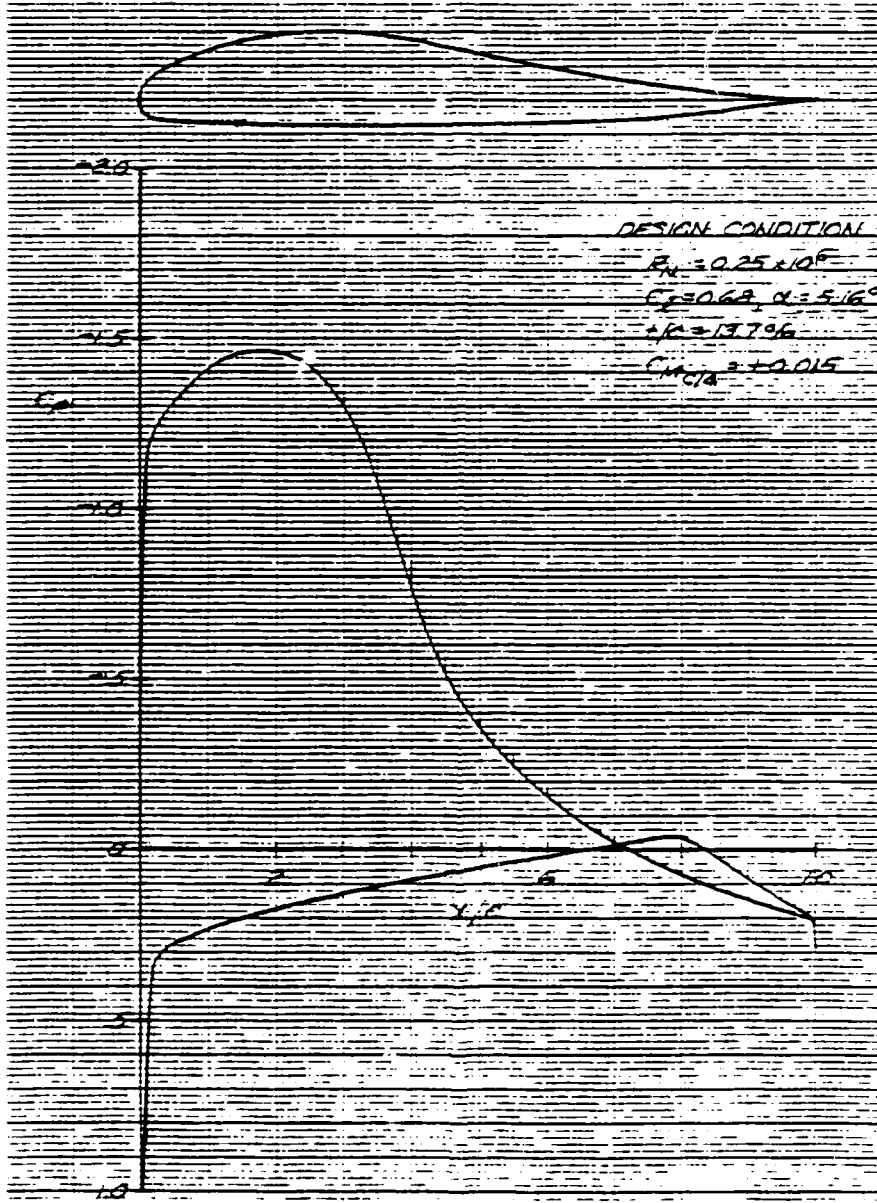


Figure 1: Airfoil LA2573A contour and theoretical design pressure distribution.
 (From R. H. Liebeck, Report #MDC18893, Douglas Aircraft Co., 1982.)

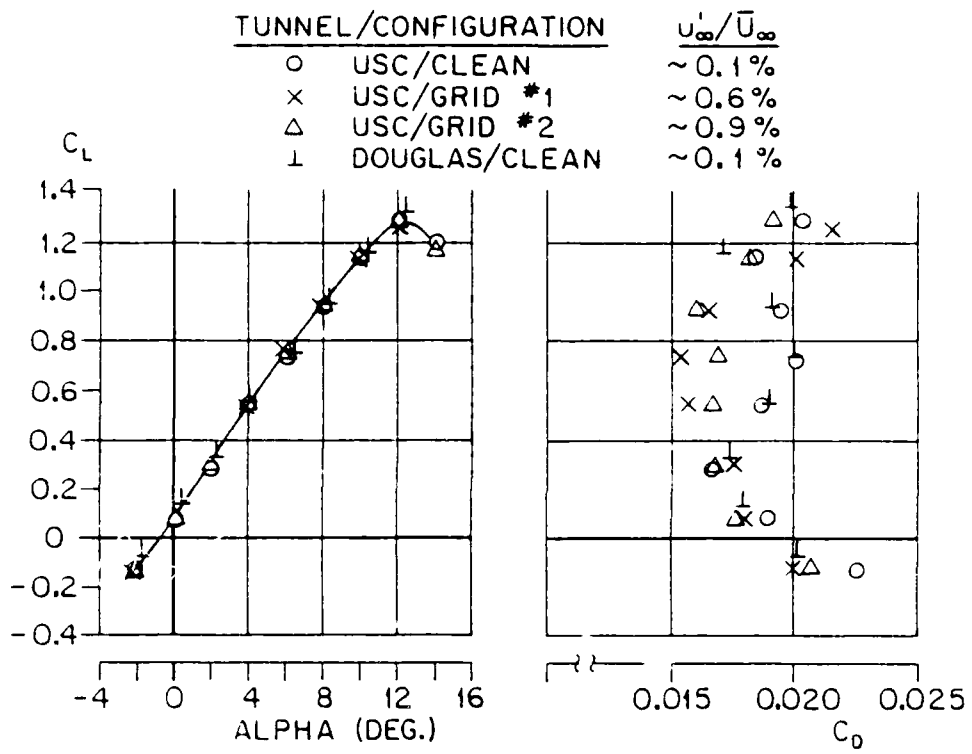


Figure 2: LA2573A airfoil performance curves at $R_c = .25 \times 10^6$.

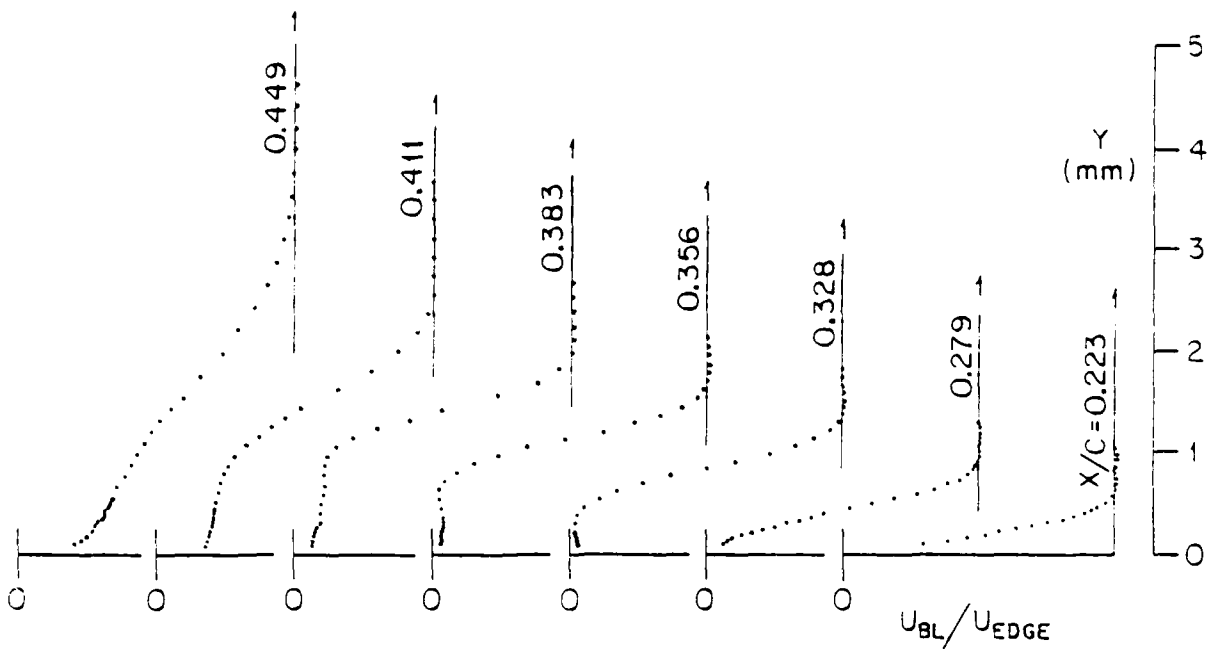


Figure 3: Mean velocity profiles: LA2573A, $R_e = .23 \times 10^6$, $\alpha = 8^\circ$.
Free stream turbulence $\approx .1\%$.

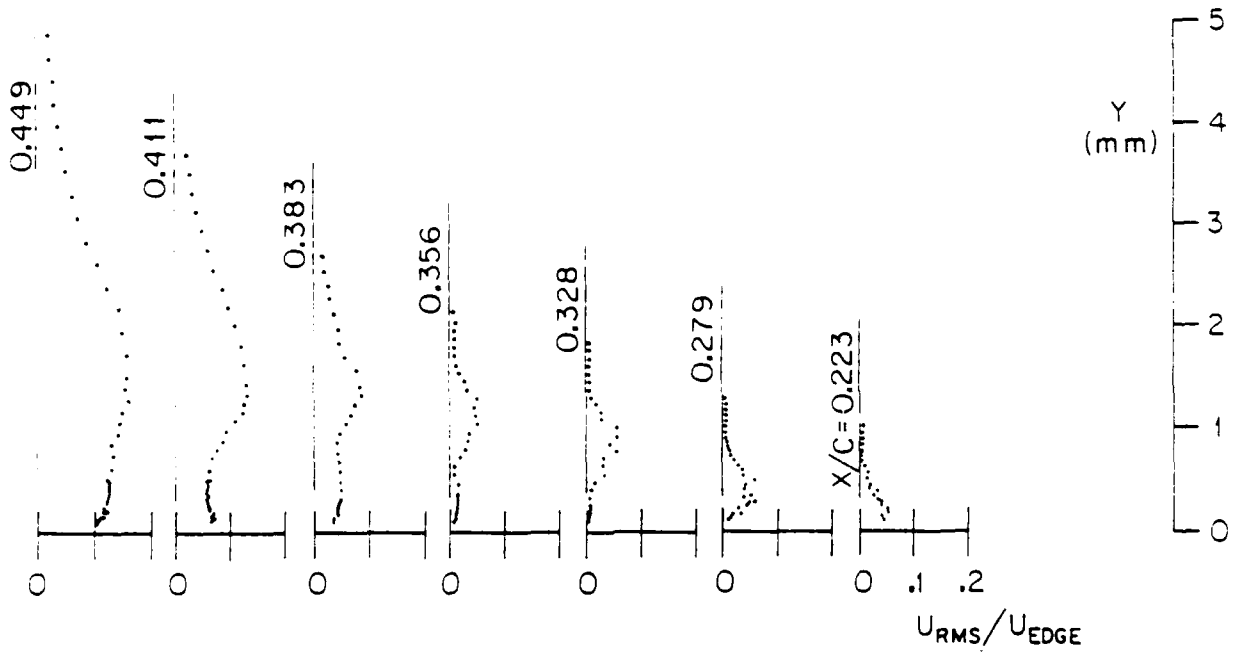


Figure 4: Turbulent intensity profiles: LA2573A, $R_e = .23 \times 10^6$, $\alpha = 8^\circ$.
Free stream turbulence $\approx .1\%$.

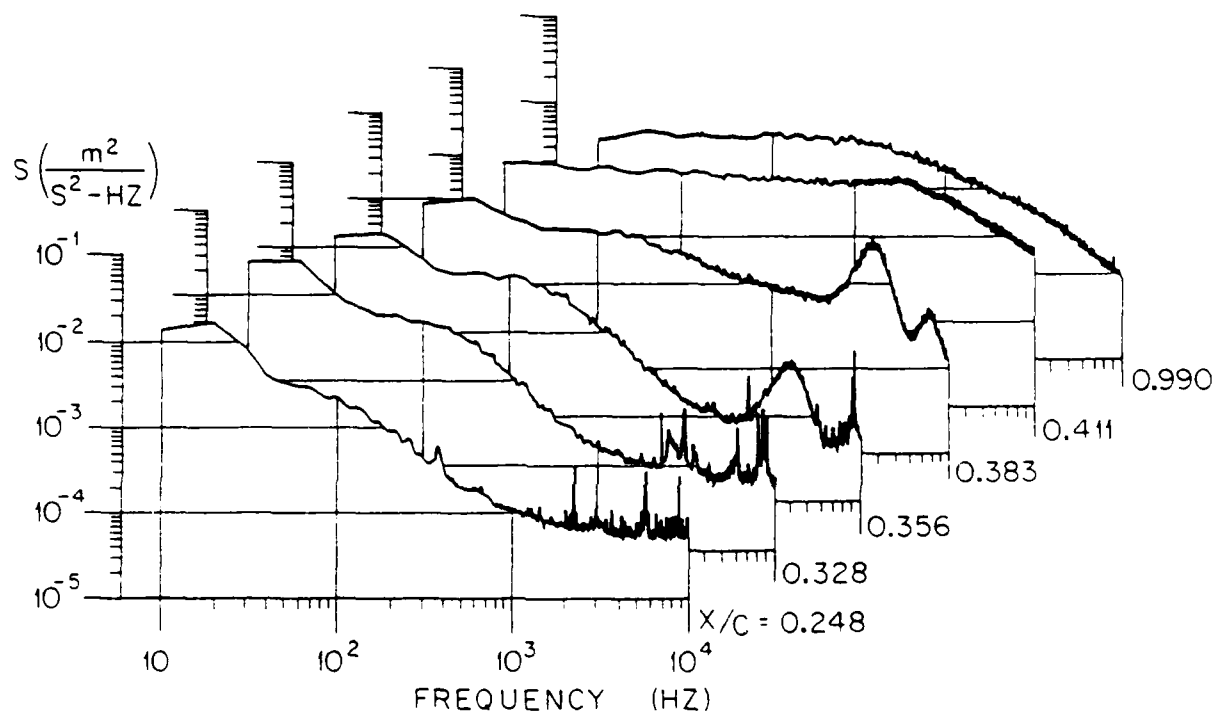


Figure 5: Boundary layer velocity spectra: LA2573A. $R_c = .23 \times 10^6$, $\alpha = 8^\circ$.
 Free stream turbulence $\approx .1\%$.
 Spectra obtained inside the boundary layer at $u \approx .7U_{edge}$.

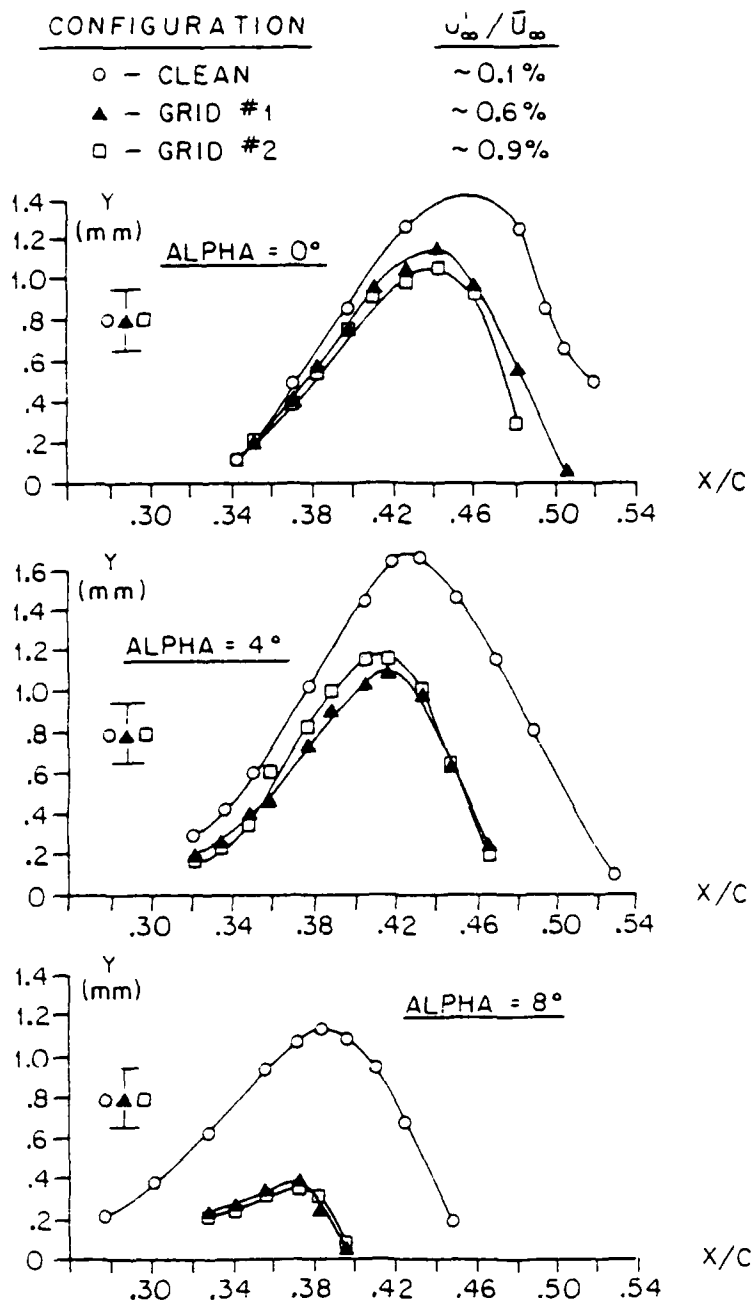


Figure 6: Separation bubble profiles at $R_c = .23 \times 10^6$.
 Normal distance from the airfoil surface: $y = y(.3U_{edge})$.

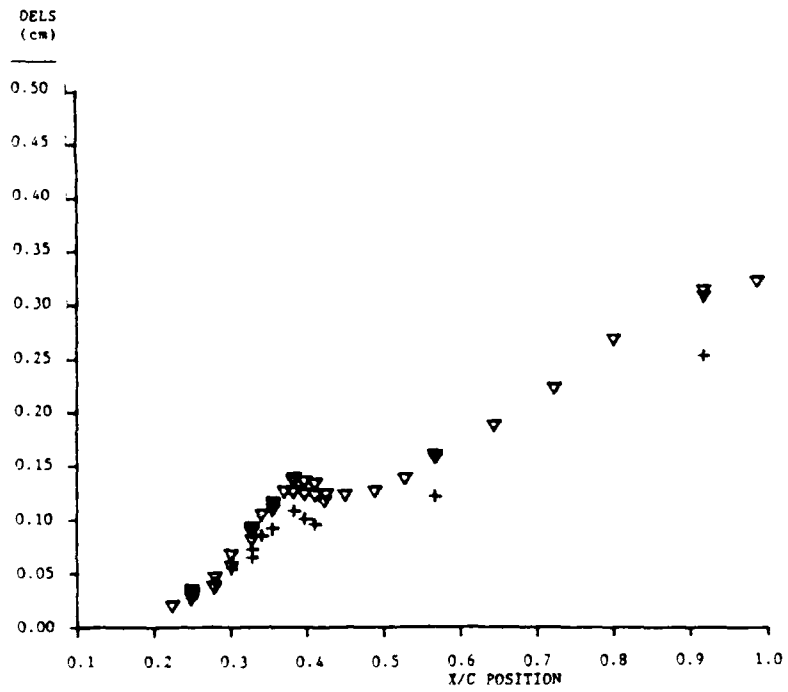


Figure 7: Boundary layer displacement thickness [DELS = δ^*].
 LA2573A: upper surface, $R_c = .23 \times 10^6$, $\alpha = 8^\circ$.

- ▽ No forcing
- + Acoustic forcing, freq. = 3.750 kHz ($A = 5.0V_{rms}$)

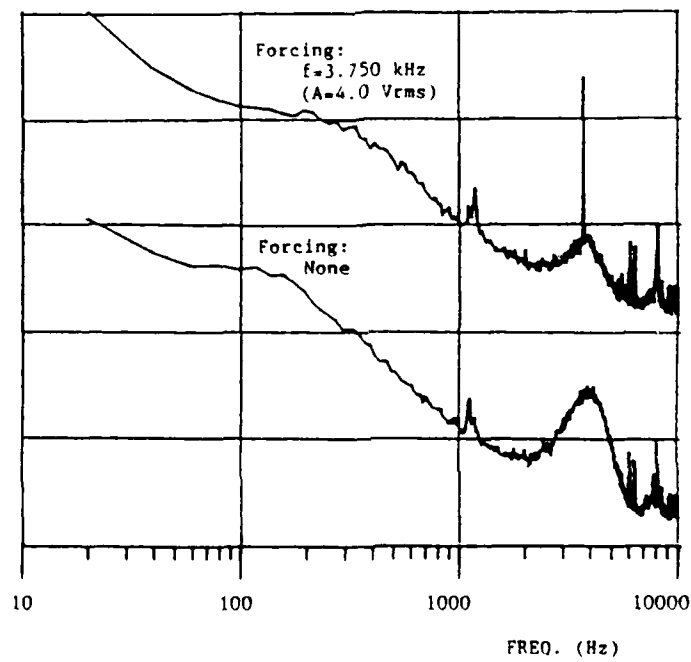


Figure 8: Boundary layer velocity spectra: LA2573A, $R_c = .23 \times 10^6$, $\alpha = 8^\circ$.
 Chord position: $x/c = .356$ (transition region).
 (Note: curves are offset by 2 vertical divisions;
 each vertical division represents a factor of 10.)